0022-3565/08/3273-727–735
THE JOURNAL OF PHARMACOLOGY AND EXPERIMENTAL THERAPEUTICS
U.S. Government work not protected by U.S. copyright
JPET 327:727–735, 2008

Vol. 327, No. 3
143347/3411023
Printed in U.S.A.

Radiodefluorination of 3-Fluoro-5-(2-(2-[^{18}F](fluoromethyl)-thiazol-4-yl)ethynyl)benzonitrile ([^{18}F]SP203), a Radioligand for Imaging Brain Metabotropic Glutamate Subtype-5 Receptors with Positron Emission Tomography, Occurs by Glutathionylation in Rat Brain

H. Umesha Shetty, Sami S. Zoghbi, Fabrice G. Siméon, Jeih-San Liow, Amira K. Brown, Pavitra Kannan, Robert B. Innis, and Victor W. Pike

Molecular Imaging Branch, National Institute of Mental Health, National Institutes of Health, Bethesda, Maryland

Received July 9, 2008; accepted September 18, 2008

ABSTRACT

Metabotropic glutamate subtype-5 receptors (mGluR5) are implicated in several neuropsychiatric disorders. Positron emission tomography (PET) with a suitable radioligand may enable monitoring of regional brain mGluR5 density before and during treatments. We have developed a new radioligand, 3-fluoro-5-(2-(2-[^{18}F](fluoromethyl)thiazol-4-yl)ethynyl)benzonitrile ([^{18}F]SP203), for imaging brain mGluR5 in monkey and human. In monkey, radioactivity was observed in bone, showing release of [^{18}F]-fluoride ion from [^{18}F]SP203. This defluorination was not inhibited by disulfiram, a potent inhibitor of CYP2E1. PET confirmed bone uptake of radioactivity and therefore defluorination of [^{18}F]SP203 in rats. To understand the biochemical basis for defluorination, we administered [^{18}F]SP203 plus SP203 in rats for ex vivo analysis of metabolites. Radio-high-performance liquid chromatography detected [^{18}F]fluoride ion as a major radiometabolite in both brain extract and urine. Incubation of [^{18}F]SP203 with brain homogenate also generated this radiometabolite, whereas no metabolism was detected in whole blood in vitro. Liquid chromatography-mass spectrometry analysis of the brain extract detected *m/z* 548 and 404 ions, assignable to the $[M + H]^+$ of *S*-glutathione (SP203Glu) and *N*-acetyl-*S*-L-cysteine (SP203Nac) conjugates of SP203, respectively. In urine, only the $[M + H]^+$ of SP203Nac was detected. Mass spectrometry/mass spectrometry and multi-stage mass spectrometry analyses of each metabolite yielded product ions consistent with its proposed structure, including the former fluoromethyl group as the site of conjugation. Metabolite structures were confirmed by similar analyses of SP203Glu and SP203Nac, prepared by glutathione *S*-transferase reaction and chemical synthesis, respectively. Thus, glutathionylation at the 2-fluoromethyl group is responsible for the radiodefluorination of [^{18}F]SP203 in rat. This study provides the first demonstration of glutathione-promoted radiodefluorination of a PET radioligand.

Metabotropic subtype-5 receptors (mGluR5) have a discrete distribution in brain and are a potential target for treating several neuropsychiatric disorders, including schizophrenia (Pietraszek et al., 2007), Alzheimer's disease (Tsai et al., 2005), anxiety (Brodkin et al., 2002), depression (Li et al., 2006), drug addiction (Kenny and Markou, 2004), and fragile X syndrome (Dölen et al., 2007). Potent noncompetitive mGluR5 antagonists, such as 6-methyl-2-(phenylethynyl)pyridine (Gasparini et al., 1999) and 3-[(2-methyl-1,3-thiazol-4-yl)ethynyl]pyridine (Cosford et al., 2003), have been developed. Nevertheless, a useful drug is yet to emerge from these antagonists for treating any of the implicated neuropsychiatric disorders. Selective imaging of mGluR5 in living human brain with a suitable radioligand and a technique such as positron emission tomography (PET) is needed to

This work was supported by the Intramural Research Program of National Institutes of Health (National Institute of Mental Health project Z01-MH-002795-04). A portion of this work was presented at the *55th American Society for Mass Spectrometry Conference on Mass Spectrometry and Allied Topics*, 2007 Jun 3–7, Indianapolis, IN.

Article, publication date, and citation information can be found at http://jpet.aspetjournals.org.

doi:10.1124/jpet.108.143347.

ABBREVIATIONS: mGluR5, metabotropic glutamate subtype-5 receptor(s); PET, positron emission tomography; SP203, 3-fluoro-5-(2-(2-(fluoromethyl)thiazol-4-yl)ethynyl)benzonitrile; [^{18}F]FCWAY, ^{18}F-*trans*-4-fluoro-*N*-(2-[4-(2-methoxyphenyl)piperazin-1-yl)ethyl]-*N*-(2-pyridyl)cyclohexanecarboxamide; [^{18}F]SP203, 3-fluoro-5-(2-(2-[^{18}F](fluoromethyl)thiazol-4-yl)ethynyl)benzonitrile; HPLC, high-performance liquid chromatography; LC-MS, liquid chromatography-mass spectrometry; MS/MS, mass spectrometry/mass spectrometry; amu, atomic mass unit(s); MS^3, multi-stage mass spectrometry; SUV, standardized uptake value; CID, collision-induced dissociation.

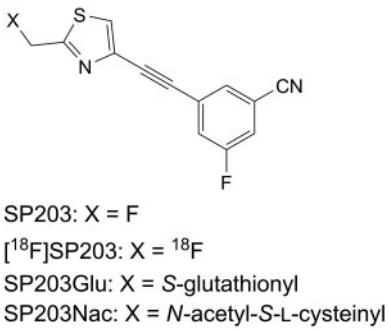

Fig. 1. Structures of SP203 and [^{18}F]SP203, their metabolites, the *S*-glutathione conjugate of SP203 (SP203Glu) and the *N*-acetyl-*S*-L-cysteine conjugate of SP203 (SP203Nac).

better elucidate the role of mGluR5 in health and neuropsychiatric disorders and thus to facilitate drug discovery.

Successful PET imaging and quantification of brain mGluR5 depends on the properties of the radioligand in vivo, especially receptor affinity, metabolism, and blood-brain barrier permeability (Pike, 1993; Laruelle et al., 2003). We have discovered a high-affinity ligand, SP203 (Fig. 1) and carried out labeling with [^{18}F]fluoride ion in one step from its bromomethyl analog to generate [^{18}F]SP203 (Lazarova et al., 2007; Sharma and Lindsley, 2007; Siméon et al., 2007). PET evaluation of [^{18}F]SP203 in monkey demonstrated that a high proportion of radioactivity in brain was bound to mGluR5. However, radioactivity also accumulated in bone, showing metabolism and release of [^{18}F]fluoride ion from [^{18}F]SP203.

The accumulation of radioactivity in bone, especially skull, would be troublesome for the quantification of mGluR5 in monkey brain, because of errors derived from the significant partial volume effects that are associated with the limited multimillimeter spatial resolution of PET. Here, we found that the radiodefluorination of [^{18}F]SP203 could not be inhibited with disulfiram, a potent inhibitor of CYP2EI, as we had shown previously to be effective for preventing the defluorination of another PET radioligand, [18F]FCWAY (Ryu et al., 2007).

The main purpose of this study was to examine the metabolism of [^{18}F]SP203/SP203 in rat so as to identify a biochemical basis for radiodefluorination of the radioligand. We conclude that nucleophilic substitution with glutathione in [^{18}F]SP203 at its [^{18}F]fluoromethyl group is responsible for releasing [^{18}F]fluoride ion.

Materials and Methods

Materials

Ascorbic acid, potassium fluoride, L-glutathione, glutathione transferase (EC 2.5.1.18), *N*-acetyl-L-cysteine, triethylamine, and buffer salts were obtained from Sigma-Aldrich (St. Louis, MO). Other materials and their sources were as follows: dehydrated ethanol USP (American Regent, Shirley, NY), silica gel (Scientific Adsorbents, Atlanta, GA), Tween 80 (Mallinckrodt Baker, Inc., Phillipsburg, NJ), Cremophor EL (BASF, Ludwigshafen, Germany), isoflurane (Baxter, McGaw Park, IL), heparin (Elkins-Sinn, Cherry Hill, NJ), heparinized tubes (VWR, West Chester, PA), and saline (American Pharmaceutical Partners, Los Angeles, CA). Solvents used for HPLC and LC-MS analyses were from Merck (EMD Chemicals, Gibbstown, NJ) or Sigma-Aldrich.

General Methods

Radiochromatographic analyses of radiometabolites in biological samples (rat brain extract, urine, or plasma) were performed on a system consisting of Gold 126 pumps and a photodiode array 168 detector (Beckman Coulter, Fullerton, CA) in-line with flow-through NaI(Tl) scintillation detector/rate meter (BioScan, Washington, DC). Data from the analyses were collected and stored on Bio-ChromeLite software (BioScan) and analyzed after decay correction. All samples were prefiltered through Nylon filters (13 mm × 0.45 μm, Iso-Disc; Supelco, Bellefonte, PA) preceding analysis. The chromatographic separation was performed on a Novapak C18 column (100 × 8 mm, within a radial compression module RCM-100; Waters, Milford, MA), eluted with methanol/water/triethylamine (80:20:0.1 by volume) at 1.5 ml/min.

LC-MS/(MS/MS) analyses were performed on a LCQ Deca MS instrument interfaced with a Surveyor HPLC pump and autosampler (Thermo Fisher Scientific, Waltham, MA). The liquid chromatography was performed with a gradient of binary solvents (A:B; 150 μl/min), composed of water/methanol/acetic acid (90:10:0.5 by volume) (A) and methanol/acetic acid [100:0.5 (v/v)] (B), on a Synergi Fusion-RP column (4 μm; 150 × 2 mm; Phenomenex, Torrance, CA). The column was equilibrated with mobile phase A:B (50% each) and upon injection, the pump ran a linear gradient reaching 20% A and 80% B over 8 min and then held this composition for 6 min. The mobile phase was returned to the initial composition and equilibrated for 2 min at 250 μl/min. After injection of sample and 2.5 min into the run, the entire column output was directed to the electrospray. Electrospray ionization was carried out with sheath and auxiliary gas flow rates of 64 and 10 units, respectively. The capillary temperature was 260°C and spray and capillary voltages were 5 kV and 21 V, respectively. A range of ions (*m/z* 150 through 600) was acquired to encompass the masses of all possible metabolites of SP203. In the MS/MS mode, the $[M + H]^+$ of SP203 or its metabolite was isolated (width, 1.5 amu) and dissociated by collision with helium at normalized collision-energy level set between 27 and 33%. The product-ion spectrum was acquired in each case. The same isolation width and collision energy levels were used for MS^3 experiments where a product ion of interest was dissociated to generate a second-order product-ion spectrum. For LC-MS analysis of stored rat brain extracts, an aliquot (1 ml) was concentrated with a SpeedVac evaporator (Thermo Fisher Scientific), and the residue was reconstituted in acetonitrile/water [50:50 (v/v); 200 μl]. Stored urine samples (200 μl) were centrifuged (10,000*g*; 1 min), and the supernatant liquid was transferred to an autosampler vial for injection into LC-MS.

^{1}H 400-MHz and ^{13}C 100-MHz NMR spectra were acquired in CD_3OD (residual solvent as reference) on an Avance 400-MHz spectrometer (Bruker, Billerica, MA), and the chemical shifts (δ) are reported in ppm down field from tetramethylsilane (δ = 0).

High-resolution mass spectra were acquired from the Mass Spectrometry Laboratory (University of Illinois at Urbana-Champaign, Urbana, IL) under electron ionization conditions using a double-focusing high-resolution mass spectrometer (AutoSpec; Micromass Inc., Beverly, MA), with samples introduced by a direct probe. Melting points were determined on a Mel-Temp manual apparatus (Electrothermal; Thermo Fisher Scientific) and were uncorrected.

Radiosynthesis of [^{18}F]SP203

[^{18}F]SP203 was prepared in an automated apparatus adapted to use microwave irradiation (Lazarova et al., 2007) by treating 3-fluoro-5-(2-(2-(bromomethyl)thiazol-4-yl)ethynyl)benzonitrile with no-carrier-added [^{18}F]fluoride ion, produced with the ^{18}O(p,n)^{18}F reaction in a PETtrace cyclotron (General Electric, Milwaukee, WI) (Siméon et al., 2007). A sample (100 μl) of each batch of [^{18}F]SP203, reconstituted in sterile saline [0.9% (w/v); 10 ml] containing ethanol [10% (v/v)], was checked for purity by HPLC analysis on a Luna C18 column (4.6 × 250 mm, 5 μm; Phenomenex), eluted with acetoni-

trile/10 mM aqueous ammonium formate [60:40 (v/v)] at 1.75 ml/min, with the eluate monitored for absorbance (λ = 310 nm) and radioactivity ([^{18}F]SP203; t_R = 5.8 min). The HPLC analysis confirmed high chemical and radiochemical purity (>99%). Specific radioactivity was calculated by relating radioactivity ([^{18}F]SP203) to the mass associated with the absorbance peak of carrier SP203. The average specific radioactivity at the end of synthesis was 9 Ci/μmol. The stability of [^{18}F]SP203 in saline and potassium fluoride solution (0.5 M) was assessed by radio-HPLC (see *General Methods*). There was no release of [^{18}F]fluoride ion from [^{18}F]SP203 by halogen exchange.

Synthesis of SP203Nac

N-Acetyl L-cysteine (6.5 mg; 40 μmol) and triethylamine (25 μl) were added to a solution of 3-fluoro-5-(2-(2-(bromomethyl)thiazol-4-yl)ethynyl)benzonitrile (3.2 mg; 10 μmol) (Siméon et al., 2007) in acetonitrile (1 ml) under argon and stirred for 15 h at 22°C. The reaction mixture was treated with aqueous acetic acid [2.5% (v/v); 4 ml] and passed through two serially connected C18 Sep-Pak cartridges (Waters). The cartridges were washed with the same acidified water (5 ml), and the retained product was eluted with acetonitrile (10 ml). The solvent was removed with a SpeedVac apparatus (Thermo Fisher Scientific), and the product was further purified by silica-gel column chromatography using ethyl acetate containing 1% (v/v) each of acetic acid and methanol as mobile phase. Thin layer chromatography (0.2-mm silica gel; Alltech Associates, Deerfield, IL) of the product with the same mobile phase showed one spot (R_f = 0.3). Evaporation of the solvent gave the product as an off-white solid, 3.7 mg (yield, 92.5%). m.p. 176–178°C. ^{1}H NMR: δ 2.01 (s, 3H), 2.90–2.95 (dd, J = 8.2, 13.8 Hz, 1H), 3.09–3.14 (dd, J = 4.5, 13.8 Hz, 1H), 4.09–4.19 (2d, J = 15.4 Hz, 2H), 4.60–4.63 (dd, J = 4.5, 8.2 Hz, 1H), 7.61–7.67 (m, 2H), 7.79 (m, 1H), 7.90 (s, 1H). ^{13}C NMR: 22.65, 33.97, 35.10, 53.98, 86.47 (d, J = 3.4 Hz) 87.28, 115.86 (d, J = 10.8 Hz), 117.93 (d, J = 3.41 Hz), 120.81 (d, J = 25.5 Hz), 124.25 (d, J = 23.4 Hz), 127.51 (d, J = 7.9 Hz), 132.63 (d, J = 3.34 Hz), 136.96, 162.45, 164.93, 172.06, 173.35, 174.30. LC-MS, *m/z* 404 $[M + H]^+$. High-resolution mass spectra calculated for $C_{18}H_{15}FN_3O_3S_2$ $[M + H]^+$, 404.0533; found, 404.0526.

Enzymic Synthesis of SP203Glu

A solution of SP203 (0.5 mg/ml) was prepared in dimethyl sulfoxide and mixed (50 μl) with Tris-HCl buffer (pH 7.4; 0.1 M; 1 ml) containing glutathione (1.5 mg). Glutathione transferase (10 units in 25 μl of buffer) was added, and the reaction mixture was shaken at 37°C for 1 h in the water bath incubator. The incubations were carried out in duplicate, including controls without the enzyme. Each reaction mixture was first diluted with water (1 ml) and passed immediately onto a C18 cartridge. The cartridge was washed with water (1 ml), and the retained components were eluted with methanol (3 ml). Solvent was removed with a SpeedVac apparatus, and the residue reconstituted in acetonitrile/water [50:50 (v/v); 200 μl] for LC-MS analysis.

Animal Studies

Twelve male Sprague-Dawley rats (376 ± 86 g; Taconic Farms, Germantown, NY) were used for various experiments as follows: three for PET study, two for in vitro radiometabolite analysis, three for ex vivo studies involving LC-MS analysis, and four for metabolite identification in brain homogenates. Rats were maintained under anesthesia using 1.5% isoflurane in oxygen during the experiments. Further specific procedures are detailed in each case below. One male rhesus monkey (*Macaca mulatta*; 9.5 kg) was anesthetized and prepared for PET imaging according to our routine protocol as described previously (Siméon et al., 2007). All animals were used in accordance with the Guide for Care and Use of Laboratory Animals (Clark et al., 1996), and studies were approved by the National Institute of Mental Health Animal Care and Use Committee.

PET Experiment in Monkey: Attempt to Inhibit Defluorination of [^{18}F]SP203

An anesthetized rhesus monkey was placed within a PET camera (high-resolution research tomograph; Siemens, Knoxville, TN), injected with [^{18}F]SP203 (4.51 mCi; 0.05 nmol/kg) alone, and the brain scanned, as described previously (Siméon et al., 2007). Emission data were collected in multiple sequential frames, reconstructed and processed to provide decay-corrected time-radioactivity concentration curves from brain regions of interest (striatum and cerebellum), with radioactivity expressed as percentage of standardized uptake value (%SUV), which normalizes for injected radioactivity and body weight: %SUV = (% injected activity/cm^3 of brain) × body weight (grams). The experiment was repeated in the same monkey after oral administration of disulfiram (500 mg) to inhibit the action of CYP2E1 (Ryu et al., 2007), approximately 20 h preceding radioligand injection (5.10 mCi; 0.10 nmol/kg).

PET Experiment in Rat: Confirmation of Radiodefluorination of [^{18}F]SP203

Each of three rats was anesthetized as described above and placed in a small animal PET camera (Seidel et al., 2003), intravenously injected with [^{18}F]SP203 (663 ± 58 μCi; 0.53 ± 0.25 ml; formulated as described under "Radiosynthesis of [^{18}F]SP203") via the penile vein, and scanned at the head over 60 min in multiple time frames. The accumulation of radioactivity in regions of brain structures such as striatum and thalamus and in skull and jaw (mandible plus maxilla) was monitored and expressed as %SUV versus time.

HPLC Analysis of Stability of No-Carrier-Added [^{18}F]SP203 in Rat Brain and Blood in Vitro

A blood sample (2 ml) was drawn from an anesthetized rat via cardiac puncture into a heparinized tube. Ice-cold (4°C) heparinized-saline (100 units/ml; 40 ml) was perfused through the left ventricle of the heart until perfusate, when leaving the opened right atrium, was clear of blood. The brain was excised and placed in ice-cold (4°C) heparinized saline (5 ml) in ice-cold glass tube of a tissue homogenizer (model 099C-K54; Glas-Col, Terre Haute, IN) and homogenized by three Teflon pestle plunges with a 5-min pause after each plunge.

[^{18}F]SP203 (20 μCi) was added to the brain homogenate (5 ml) and then incubated at 37°C in a reciprocating-shaker water bath (model 25; Precision Scientific, Chicago, IL) at 60 oscillations/min. Aliquots (50 μl) from the incubation mixture were removed at 5, 10, 15, 30, and 60 min, placed in acetonitrile (300 μl) that had been spiked with SP203, and then mixed. Potassium fluoride solution (0.5 M; 50 μl) was added, and the solution was mixed again. All samples were measured in a gamma counter and then centrifuged at 10,000*g* for 1 min. The supernatant liquids were analyzed by radio-HPLC (see *General Methods*). The precipitates were then counted in a gamma counter for calculating the recovery of radioactivity into the acetonitrile.

In a separate experiment, rat brain homogenates were incubated with [^{18}F]SP203 for 1.5 h, and then they were analyzed simultaneously on two chromatographic systems to separate and identify radiometabolite. One system was that described under *Materials and Methods*. The other was based on the use of a Shodex ODP2 HP-4E column (250 × 4.6 mm, 5 μm; Showa Denko America, Inc., New York, NY). The Shodex column has mixed mode features (size exclusion and polymer-based stationary phase) that allow polar compounds, such as [^{18}F]fluoride ion, to be retained when acetonitrile predominates in the mobile phase. Thus, the column was equilibrated with acetonitrile/100 mM ammonium formate [80:20 (v/v); pH 4.5] at 0.7 ml/min. All samples were deproteinized with acetonitrile and adjusted to a final acetonitrile composition of 80%. Up to 1 ml of the biological sample could be injected onto the Shodex column. Potassium fluoride solution (>0.5 mM; 100 μl) was added to enhance separation of [^{18}F]fluoride ion (t_R = 10.4 min) from unchanged [^{18}F]SP203 (t_R = 1.8 min) on the Shodex column.

For blood analysis, sample (2 ml) was mixed with [^{18}F]SP203 (3.5 μCi) in a polypropylene tube (13 × 60 mm) and incubated at 37°C, as described above. A 50-μl aliquot of the radioactive blood was removed at 5, 10, 15, 30, and 60 min and placed in saline (1 ml) and centrifuged (1800*g*; 1.5 min). The supernatant plasma-saline was separated from the pelleted cells. The cell and plasma-saline fractions were mixed first with acetonitrile (300 μl) that had been spiked with SP203 and then with potassium fluoride solution (0.5 M; 50 μl). The samples were measured in a gamma counter and centrifuged (10,000*g*; 1 min), and the supernatant liquids were injected onto radio-HPLC for analysis. The precipitates were then measured in a gamma counter to calculate recovery of radioactivity into the acetonitrile.

Ex Vivo Measurements of Carrier-Added [^{18}F]SP203 or SP203 and Metabolites in Rat Urine and Brain

Carrier-Added [^{18}F]SP203. A dose of carrier-added [^{18}F]SP203 (617 μCi; 4.7 μmol/kg) was formulated with Cremophor EL (35 mg), ascorbic acid (100 μg) in saline [sodium chloride, 0.9% (w/v); 1 ml] containing ethanol [15% (v/v)]. One rat was maintained under anesthesia, and the entire dose of [^{18}F]SP203 was injected through the penile vein over a period of 3.5 min. The animal's urethra was clamped, and every 10 min, a dose of saline (0.3 ml) was injected to ensure expression of urine. At the end of 60 min, the urinary bladder of the rat was exposed, and urine (1.1 ml) was withdrawn into a syringe.

The same rat was perfused with heparinized saline (12 ml) to rid the brain of circulating blood as described above. The brain (1.7 g) was then excised, placed in acetonitrile (3 ml), and homogenized (Tissue Tearor model 985-370; BioSpec Products; Bartlesville, OK). Water (500 μl) was added, the sample was homogenized once more, and the resulting brain homogenate was centrifuged (10,000*g*; 10 min). The clear supernatant was decanted into a polypropylene tube (4 ml). The precipitate was rehomogenized with acetonitrile followed by water and then centrifuged as described above. The second supernatant liquid was combined with the first supernatant liquid.

Aliquots from the urine and brain-acetonitrile extract were immediately analyzed by radio-HPLC. The remaining samples were stored at −70°C until LC-MS analysis.

SP203 Alone. A dose of SP203 (3.15 mg) was formulated for injection by dissolution in ethanol (400 μl) plus Tween 80 (100 μl) and then dilution to 2.0 ml with saline. Each rat was infused through the penile vein with saline (3 ml) for 30 min followed by the entire dose of SP203 for another 30 min. The infusion was continued with saline (2.0 ml) for another 30 min. At the end of the experiment, the urinary bladder of the rat was exposed, and urine (3.0 ml) was withdrawn into a syringe. The brain (1.6 g) was excised, homogenized with acetonitrile/water, and centrifuged as described above. The brain-acetonitrile extracts and urine samples were immediately stored at −70°C until LC-MS analysis.

LC-MS Investigation of SP203 Metabolites from Rat Brain Homogenate in Vitro

Rats were anesthetized, and their brains (1.7 g each) were harvested and placed immediately in glass vials on ice. Ice-cold saline (4 ml) was added to each brain and then homogenized (Tissue Tearer; BioSpec Products) with short durations of homogenizing pulses (with pauses to cool) while the vial was on ice. Each brain homogenate was divided into two equal volumes. The substrate SP203 (1.6 mg; 6.15 μmol) was formulated by dissolving it in ethanol (200 μl). Tween 80 (25 μl) was added, and the solution was diluted to 800 μl with saline. From this solution, a 200-μl aliquot (1.54 μmol) was added to each of the four brain homogenate samples. The vials were then incubated at 37°C for 90 min, as described above. At the end of the incubation, acetonitrile (4 ml) followed by water (500 μl) was added to each brain fraction, and the samples were mixed again. The homogenates were then transferred to polypropylene tubes (15-ml size) and centrifuged at 10,000*g* for 5 min. The clear supernatant liquids were transferred to another set of polypropylene tubes.

The acetonitrile extract from the incubation of SP203 with brain homogenate was concentrated until most of the acetonitrile had been evaporated off. The remaining aqueous layer was diluted with water (2 ml) and passed through a C18 cartridge (Waters). The cartridge was washed with water (3 ml), and the retained components were eluted with methanol (3 ml). The solvent was removed by evaporation, and the residue reconstituted in acetonitrile-water [50:50 (v/v); 200 μl] for LC-MS analysis.

Results

PET Experiment in Monkey: Attempt to Inhibit Defluorination of [^{18}F]SP203 in Monkey. Thirty minutes after the injection of [^{18}F]SP203 into monkey, brain peak activity was approximately 725% SUV, which declined by half in 180 min after injection. Dosing monkey with the potent CYP2E1 inhibitor disulfiram (500 mg), at ~20 h preceding administration of [^{18}F]SP203, had no effect on the accumulation of radioactivity in bone, as represented by jaw (Fig. 2). In this experiment, conducted in a single monkey, the uptake of radioactivity into brain regions, however, was increased, namely, by 58 and 21% for area under curves (0–180 min) for striatum and cerebellum, respectively.

PET Experiment in Rat: Confirmation of Radiodefluorination of [^{18}F]SP203. PET imaging of rat injected with [^{18}F]SP203 revealed continuous accumulation of radioactivity in skull and jaw (Fig. 3). The time-activity curve of the brain regions showed high uptake of radioactivity (~300% SUV) (Fig. 3), which persisted throughout the duration (60 min) of the experiment. The corresponding summed PET images clearly showed the high uptake of radioactivity into skull and jaw (Fig. 4).

Stability of [^{18}F]SP203 in Rat Blood and Brain Homogenate in Vitro. After incubation of [^{18}F]SP203 with rat blood, 35 ± 3.9% (mean ± S.D.; n = 7) of the radioactivity distributed to blood cells and the remainder to plasma. [^{18}F]SP203 was stable both in plasma and blood cells but not in brain homogenate. Acetonitrile extraction of plasma and cell fractions recovered 99.0 ± 1.1% (n = 7) and 93.3 ± 1.2% (n = 6) of the radioactivity, respectively. Radio-HPLC anal-

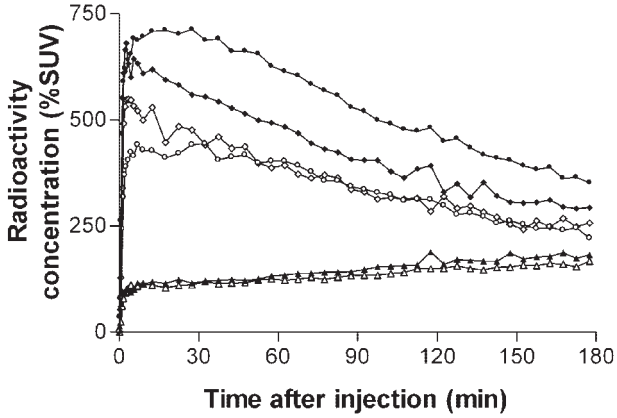

Fig. 2. Time course for the uptake of radioactivity into striatum, cerebellum, and jaw of rhesus monkey after the intravenous injection of [^{18}F]SP203 alone (4.51 mCi; 0.05 nmol/kg) and [^{18}F]SP203 (5.10 mCi; 0.10 nmol/kg) ~20 h after the administration of disulfiram (500 mg orally). Striatum at baseline (○); cerebellum at baseline (◇); jaw at baseline (△); striatum after disulfiram (■); cerebellum after disulfiram (◆); and jaw after disulfiram (▲).

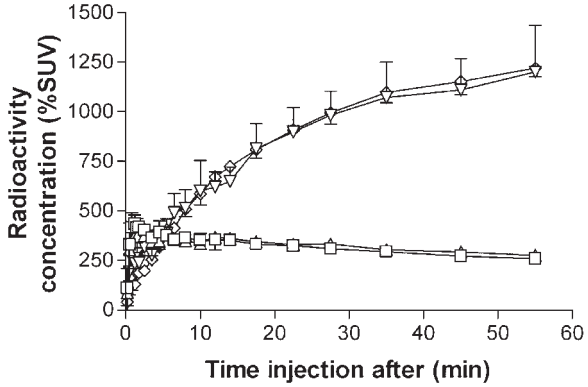

Fig. 3. Time course for the uptake of radioactivity into skull (▽), jaw (◇), thalamus (□), and putamen (△) after the intravenous injection of [^{18}F]SP203 (663 ± 58 μCi) into rat. Each data point represents mean ± S.D. values from three animals. Deep gray matter structures were chosen to illustrate brain uptake while avoiding spillover contamination from the radioactivity of the skull. Extensive radiodefluorination is evident by the continuous accumulation of radioactivity (%SUV) in the skull and jaw.

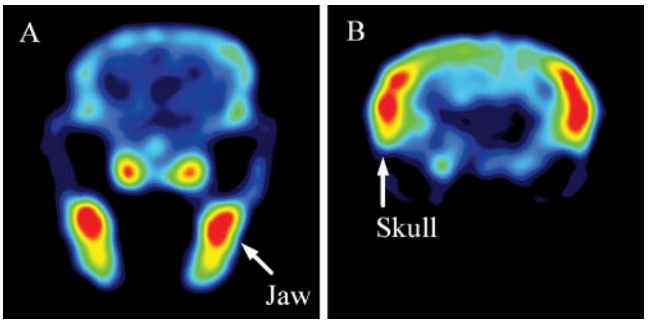

Fig. 4. PET images of a rat head reconstructed from the entire 60 min of emission data after intravenous injection of [^{18}F]SP203. High radioactivity uptake into the jaw (A) and skull (B) can be clearly seen.

ysis showed no significant metabolism of [^{18}F]SP203 in either of these fractions of the blood over 60 min.

Incubation of [^{18}F]SP203 with brain homogenate for various periods and extraction of each incubation mixture (potassium fluoride added) with acetonitrile recovered 92.0 ± 2.9% (n = 7) of the radioactivity. Reverse phase radio-HPLC of the incubation mixture on the Novapak C18 column (see *General Methods*) revealed a major radiometabolite eluting at t_R = 2.1 min (void volume) and the unchanged [^{18}F]SP203 eluting at t_R = 5.08 min. Radiometabolite and [^{18}F]SP203 eluted in reverse order on the Shodex column but in the same relative amounts. The radiometabolite had the same retention time as that of cyclotron-produced [^{18}F]fluoride ion, thereby verifying its identity. Approximately 50% [^{18}F]SP203 was biotransformed into [^{18}F]fluoride ion in brain homogenate within 20 min of incubation.

Radio-HPLC Analysis of Rat Brain Extract and Urine after Administration of Carrier-Added [^{18}F]SP203 in Vivo. Acetonitrile extraction of brain from a single rat infused with carrier-added [^{18}F]SP203 recovered 53.4% of radioactivity. Radio-HPLC of the brain extract showed a polar radiometabolite peak at the void volume and another peak for unchanged [^{18}F]SP203. The ratio of radiometabolite to [^{18}F]SP203 radioactivity at 60 min after radioligand injection was 10:1. Similar analysis of rat urine at 60 min after radioligand injection showed the same radiometabolite peak containing 97% of all radioactivity, with the remainder represented by unchanged [^{18}F]SP203.

Ex Vivo LC-MS Analysis of Rat Brain Extract and Urine from Rat Administered with Carrier-Added [^{18}F]SP203 or SP203 Alone. The brain extracts from each rat administered with carrier-added [^{18}F]SP203 or SP203 alone were analyzed by LC-MS. A knowledge-based search of metabolite-specific ions in the total-ion chromatogram identified a peak (t_R = 5.8 min) for m/z 548 ion and another (t_R = 8.7 min) for m/z 404 ion. These metabolite-specific ions were absent in brain extract and urine from a control rat. The $[M + H]^+$ ion at m/z 548 was hypothesized to correspond to the $[M + H]^+$ ion of a structure in which glutathione is bonded to SP203 by displacing fluoride ion (SP203Glu; Fig. 1). The ion-chromatogram and mass spectrum for this metabolite are shown in Fig. 5A. The second metabolite with $[M + H]^+$ at m/z 404 was hypothesized to be due to the $[M + H]^+$ ion of an *N*-acetyl L-cysteine conjugate of SP203 (SP203Nac; Fig. 1). The ion-chromatogram and mass spectrum for this brain metabolite are shown in Fig. 6A.

MS/MS analysis of the rat brain extract involving trapping and collision-induced dissociation (CID) of each of m/z 548 and m/z 404 ions, generated product-ion spectra as shown in Figs. 5B and 6B, respectively. The fragmentation pathways proposed for the $[M + H]^+$ ions of the putative SP203Glu and SP203Nac metabolites are shown in Figs. 7 and 8, respectively.

LC-MS analysis of urine samples from these experiments

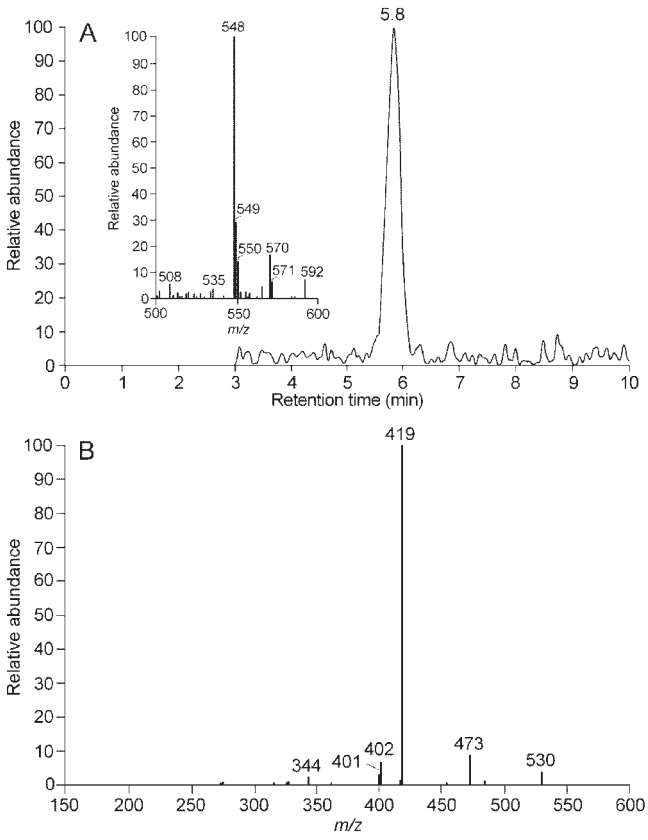

Fig. 5. LC-MS/(MS/MS) analysis of the metabolite SP203Glu in brain extract from rat infused with SP203: mass spectrum (inset) showing $[M + H]^+$ at m/z 548 and the ion chromatogram for the same ion (A); product-ion spectrum generated by CID of m/z 548 ion (B).

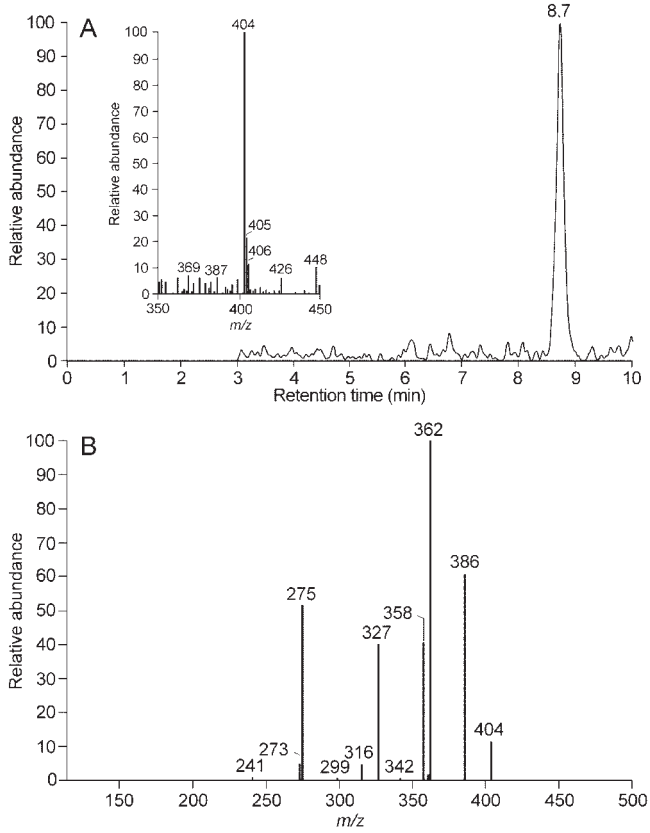

Fig. 6. LC-MS/(MS/MS) analysis of the metabolite SP203Nac in brain extract from rat infused with SP203: mass spectrum (inset) showing $[M + H]^+$ at *m/z* 404 and the ion chromatogram for the same ion (A); product-ion spectrum generated by CID of *m/z* 404 ion (B).

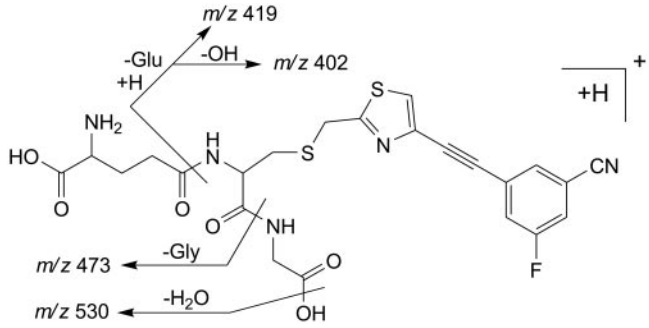

Fig. 7. Proposed fragmentation pathway for ions formed by CID of $[M + H]^+$ *m/z* 548 of SP203Glu. The fragmentation accounts for the major ions in the product-ion spectrum of SP203Glu (see Fig. 5B).

showed an intense *m/z* 404 peak with the same t_R as that of the putative SP203Nac in brain, which generated a product-ion spectrum matching that of the brain extract. The peak for *m/z* 548 ion seen in brain was not detected in the total ion-chromatogram from urine.

LC-MS/MS and MS³ Confirmation of Metabolite Identities. The LC-MS/MS characteristics of authentic SP203Nac, prepared by nucleophilic substitution in 3-fluoro-5-(2-(2-(bromomethyl)thiazol-4-yl)ethynyl)benzonitrile with *N*-acetyl-L-cysteine, were in complete agreement with those of the putative SP203Nac metabolite, thereby confirming its identity. Likewise, the product of incubation of SP203 with glutathione and glutathione transferase showed a peak for *m/z* 548 ion at the same HPLC retention time as that of SP203Glu, the metabolite of SP203 generated in rat brain. The CID of this enzymically generated standard showed all the product ions characteristic of putative SP203Glu metabolite.

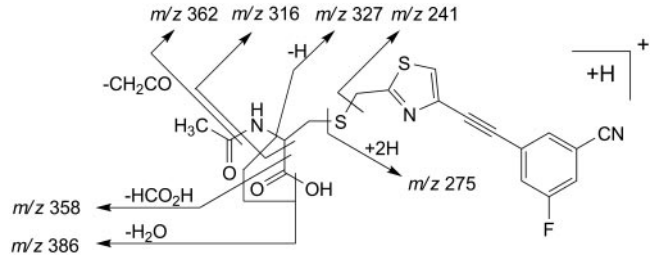

Fig. 8. Proposed fragmentation pathway for ions formed by CID of $[M + H]^+$ *m/z* 404 of SP203Nac. The fragmentation accounts for the major ions in the product-ion spectrum of SP203Nac (see Fig. 6B).

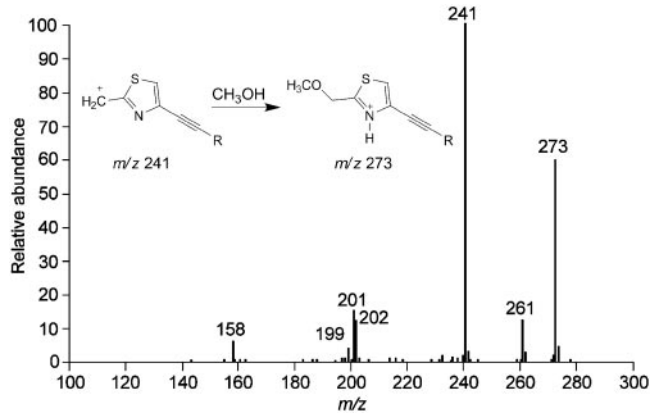

Fig. 9. Product-ion spectrum generated by CID of $[M + H]^+$ *m/z* 261 of SP203 and proposed structure (inset) of adduct-ion *m/z* 273 formed by addition of methanol to *m/z* 241 ion (R is 3-fluoro-5-cyanophenyl). The methanol-adduct formation provided additional proof for the site of glutathione conjugation in SP203Glu.

To verify the site of conjugation in SP203 metabolites to be the former fluoromethyl group, MS^3 experiments were performed on SP203Nac and SP203Glu. Thus, CID of $[M + H]^+$ (*m/z* 404) of SP203Nac followed by its product ion *m/z* 275 (Fig. 6B) generated a secondary product-ion spectrum (data not shown) with fragment ion *m/z* 241 and the methanol-adduct ion *m/z* 273, as observed with the CID of $[M + H]^+$ of SP203 (Fig. 9). These two ions also were observed in the secondary product-ion spectrum of SP203Glu generated by dissociating the product ion *m/z* 419 (Fig. 5B).

Identification of the Metabolites of SP203 Generated in Brain Extract in Vitro. LC-MS analysis of metabolites extracted from the incubation of SP203 with rat brain homogenate showed $[M + H]^+$ at *m/z* 548 due to SP203Glu. CID of this ion showed the same product ions as those obtained from the analysis of brain SP203Glu from the experiment in vivo. The same incubation mixture showed a very weak peak for the *m/z* 404 ion. However, its CID generated all product ions characteristic of SP203Nac.

Discussion

This study establishes glutathionylation as the mechanism of radiodefluorination of [^{18}F]SP203 in rat brain. The same metabolic pathway is also significant in the periphery.

[^{18}F]SP203 readily entered monkey brain because of its moderate lipophilicity (log P = 2.18) (Siméon et al., 2007).

This radioactivity washed out of the brain, suggesting metabolic stability of the radioligand in the monkey brain. In an attempt to inhibit radiodefluorination, pretreatment with disulfiram increased (20–60%) brain uptake of [^{18}F]SP203 radioactivity (Fig. 2), possibly, consequent to decreased metabolic clearance and elevation of [^{18}F]SP203 in the plasma input function. However, radiodefluorination was not eliminated, thereby suggesting the involvement of defluorination mechanisms other than those mediated by CYP2E1. We wanted to elucidate the mechanism of [^{18}F]SP203 radiodefluorination, because this information could perhaps open opportunities for modulation of this process and also assist in future PET radioligand design. Thus, the metabolism of [^{18}F]SP203 and SP203 was further investigated in rats under experimental conditions relevant to PET studies.

In PET experiments with ^{18}F-labeled tracers, radioactivity uptake into bones, including skull, is direct evidence of radiodefluorination (Tipre et al., 2006; Grant et al., 2008). In addition, bones do not take up and accumulate radioligands or any of their organic radiometabolites during these experiments. PET imaging in rats revealed high radioactivity uptake into bone (skull and jaw) (Figs. 3 and 4), confirming peripheral radiodefluorination of [^{18}F]SP203. The radioactivity within brain remained steady, consistent with biotransformation of [^{18}F]SP203 into [^{18}F]fluoride ion and its retention in the brain. The brain entrapment of radioactivity with no washout, unlike in the monkey brain, is a strong indication of extensive defluorination of [^{18}F]SP203 inside the rat brain. [^{18}F]SP203 was found to be radiochemically stable in rat plasma and blood cells in vitro but to be readily metabolized in brain homogenate. Only one radiometabolite was generated. The properties of this radiometabolite were those expected for [^{18}F]fluoride ion, especially elution at the solvent front on reverse phase HPLC, regardless of elution conditions, and improved recovery for analysis in the presence of carrier fluoride ion. Radiochromatography on a Shodex ODP2 HP-4E column confirmed that the radiometabolite was [^{18}F]fluoride ion.

HPLC analysis of rat brain extract and urine from rat infused with [^{18}F]SP203 also revealed [^{18}F]fluoride ion as the single major radiometabolite, thereby showing that defluorination was occurring in periphery as well as in brain. That is, virtually all [^{18}F]fluoride ion generated in brain would be retained there because of its charge for the duration of our experiments. A complete characterization of nonradioactive metabolites was needed to understand the metabolic basis for the release of [^{18}F]fluoride ion from [^{18}F]SP203. Accordingly, we infused rats with [^{18}F]SP203 plus carrier SP203 or with SP203 alone to enable screening of metabolites by LC-MS methods.

The metabolism of 3-[(2-methyl-1,3-thiazol-4-yl)ethynyl]-pyridine, an mGluR5 antagonist structurally related to SP203, has been examined in mouse liver microsomal preparations (Yang and Chen, 2005). In this in vitro study, the metabolites are formed by cytochromes P450-mediated reactions, i.e., hydroxylation of the 2-methyl group, and *N*-oxidation and epoxidation of the thiazole ring. The analogous SP203 metabolites from such pathways were not detected in brain or urine of rats infused with SP203. We did not examine the SP203 metabolism in liver microsomal preparations, as such in vitro data cannot be readily extrapolated to PET experimental conditions. In the present study, LC-MS analysis of the rat brain extract and urine detected no metabolites of SP203 derived from oxidative-defluorination reactions, although such reactions have been observed for other alkyl fluorides (Burke et al., 1981; Teitelbaum et al., 1981; Ma et al., 2001). Data from radiochromatography and LC-MS analysis are consistent with defluorination by glutathionylation as the major pathway for the metabolism of SP203 in rat.

In brain, the glutathione/glutathione transferase system plays a pivotal role in the removal of free radicals and reactive electrophilic species (Baez et al., 1997; Dringen, 2000; Sidell et al., 2003). Glutathione transferase is known to dehalogenate certain alkyl iodides, bromides, and chlorides (Ridgewell and Abdel-Monem, 1987; Wheeler et al., 2001) by incorporating glutathione. Generally, alkyl fluorides are not regarded as good substrates for this enzyme. In rats, fluoroacetate undergoes defluorination by a fluoroacetate-specific dehalogenase, and the role of glutathione transferase in the reaction is unclear (Tecle and Casida, 1989; Soiefer and Kostyniak, 1984; Tu et al., 2005). The basis for metabolic defluorination of certain benzyl fluorides, structurally analogous to fluoromethyl-thiazolyl moiety in SP203, is not known (Magata et al., 2000).

If SP203 undergoes defluorination by glutathionylation, its glutathione conjugate is expected to be present in the brain extract of the rat infused with SP203. Accordingly, the metabolite-specific ion, the $[M + H]^+$ of SP203Glu, was searched for and identified from the LC-MS total-ion chromatogram for the brain extract (Fig. 5). The MS/MS analysis aided the identification of this metabolite as the glutathione adduct of SP203 (Fig. 5). The product-ion spectrum showed *m/z* 530, 473, and 419 ions corresponding to loss of H_2O, glycine, and glutamate species, respectively, from the $[M + H]^+$ at *m/z* 548. This fragmentation pattern (Fig. 7) is comparable with that of glutathione conjugates of other xenobiotics (Grillo et al., 2003; Chen et al., 2006). The structure of SP203Glu was verified by treating SP203 with glutathione plus glutathione transferase and showing by MS/MS analysis that the product was the same as the conjugate identified in rat brain ex vivo. Incubation of SP203 with rat brain homogenate also yielded SP203Glu, consistent with the proposal that the synthesis of SP203Glu occurs within brain when the animal is infused with SP203.

Reactive xenobiotics and metabolites undergo glutathionylation efficiently in liver where glutathione transferase isozymes and glutathione are present in high concentrations (Commandeur et al., 1995; Rinaldi et al., 2002). Once formed, the glutathione conjugates are transported out of the cells and released to the circulation for eventual elimination. In kidney and possibly in other organs, these metabolites are further biotransformed to *N*-acetyl L-cysteine derivatives (mercapturic acids) and then excreted (Commandeur et al., 1995).

Likewise, SP203 can enter the mercapturic acid pathway in various organs, resulting in synthesis of SP203Glu and its eventual biotransformation to the end-metabolite SP203Nac. When the urine from SP203-infused rat was analyzed by LC-MS, a very intense peak for *m/z* 404 ion corresponding $[M + H]^+$ of SP203Nac was observed in the total-ion chromatogram. Its CID-generated product ions account for cleavage at the thioether bonds and at other bonds that result in loss of neutral species such as H_2O, HCO_2H, and CH_2CO (Fig. 8).

The fragmentation pattern is consistent with the proposed structure of SP203Nac wherein *N*-acetyl L-cysteine residue is linked via a thioether bond to the former 2-fluoromethyl group of SP203, replacing the fluorine. For confirmation of its structure, SP203Nac was synthesized and showed the same product-ion spectrum as that of the metabolite, putatively identified as SP203Nac. Thus, peripheral SP203Glu is formed by displacing fluoride ion from SP203, consistent with the proposed urinary excretion of radiometabolite [^{18}F]fluoride ion in rats administered [^{18}F]SP203.

In SP203-infused rats, the urinary metabolite SP203Nac was also found in brain, thereby showing further metabolism of SP203Glu within brain and/or entry of SP203Nac from the periphery. Plasma was not analyzed to determine the source of this secondary metabolite in brain. However, incubation of SP203 with brain homogenate generated SP203Nac showing that enzymes in brain are capable of converting SP203Glu into SP203Nac. Indeed, mammalian brains are known to have the enzymes of the mercapturic acid pathway capable of biotransforming reactive xenobiotics into their *N*-acetyl cysteine conjugates (Montine et al., 2000; Sidell et al., 2003).

In rats, biotransformation of SP203 into SP203Glu involving displacement of fluoride ion explains the emergence of one major radiometabolite in brain when [^{18}F]SP203 is administered intravenously. The peripheral organs also carry out this reaction as evident from excretion of mercapturic acid SP203Nac into the urine. Characterization of SP203Glu and SP203Nac provided definitive, indirect evidence for [^{18}F]fluoride ion as being the radiometabolite of [^{18}F]SP203. Additionally, it allowed us to propose that [^{18}F]fluoride ion generated in peripheral organs is the source of skull radioactivity observed in rats infused with [^{18}F]SP203. Defluorination by glutathionylation of [^{18}F]SP203 seems to be highly efficient in the rat. This makes rat unsuitable as an animal model for PET quantification of brain mGluR5.

The utility of [^{18}F]SP203 in PET imaging of brain mGluR5 in human subjects is currently being evaluated. The mammalian glutathione transferases exhibit species and tissue variations in their activity (Lash et al., 1998; Bogaards et al., 1999; Cannady et al., 2006). In general, human glutathione transferases show significantly lower activity than the rat enzymes for incorporating glutathione into reactive xenobiotics. Perhaps for this reason, our initial studies with [^{18}F]SP203 in human subjects show only limited defluorination. Thus, [^{18}F]SP203 is proving a useful radioligand for PET imaging of brain mGluR5 in humans (Brown et al., 2008). The current study provides the first demonstration of glutathionylation as a mechanism for PET radioligand defluorination in vivo. This mechanism will need to be taken into account in the design of future ^{18}F-labeled PET radioligands.

Acknowledgments

We thank Andrew Taku and Edward Tuan for help in radiosynthesis and radiometabolite analysis, respectively.

References

Baez S, Segura-Aguilar J, Widersten M, Johansson AS, and Mannervik B (1997) Glutathione transferases catalyse the detoxication of oxidized metabolites (o-quinones) of catecholamines and may serve as an antioxidant system preventing degenerative cellular processes. *Biochem J* **324:**25–28.

Bogaards JJ, Venekamp JC, Salmon FG, and van Bladeren PJ (1999) Conjugation of isoprene monoepoxides with glutathione, catalyzed by alpha, mu, pi and theta-class glutathione *S*-transferases of rat and man. *Chem Biol Interact* **117:**1–14.

Brodkin J, Busse C, Sukoff SJ, and Varney MA (2002) Anxiolytic-like activity of the mGluR5 antagonist MPEP: a comparison with diazepam and buspirone. *Pharmacol Biochem Behav* **73:**359–366.

Brown AK, Kimura Y, Zoghbi SS, Siméon FG, Liow J-S, Kreisl WC, Taku A, Fujita M, Pike VW, and Innis RB (2008) Metabotropic glutamate subtype-5 (mGluR5) receptors quantified in human brain with a novel radioligand for positron emission tomography. *J Nucl Med* DOI:10.2967/jnumed.108.056291.

Burke TR Jr, Branchflower RV, Lees DE, and Pohl LR (1981) Mechanism of defluorination of enflurane. Identification of an organic metabolite in rat and man. *Drug Metab Dispos* **9:**19–24.

Cannady EA, Chien C, Jones TM, and Borel AG (2006) In vitro metabolism of the epoxide substructure of cryptophycins by cytosolic glutathione *S*-transferase: species differences and stereoselectivity. *Xenobiotica* **36:**659–670.

Chen Q, Doss GA, Tung EC, Liu W, Tang YS, Braun MP, Didolkar V, Strauss JR, Wang RW, Stearns RA, et al. (2006) Evidence for the bioactivation of zomepirac and tolmetin by an oxidative pathway: identification of glutathione adducts in vitro in human liver microsomes and in vivo in rats. *Drug Metab Dispos* **34:**145–151.

Clark JD, Baldwin RL, Bayne KA, Brown MJ, Gebhart GF, Gonder JC, Gwathmey JK, Keeling ME, Kohn DF, Robb JW, et al. (1996) *Guide for the Care and Use of Laboratory Animals*, National Academies Press, Washington, DC.

Commandeur JN, Stijntjes GJ, and Vermeulen NP (1995) Enzymes and transport systems involved in the formation and disposition of glutathione *S*-conjugates. Role in bioactivation and detoxication mechanisms of xenobiotics. *Pharmacol Rev* **47:**271–330.

Cosford ND, Tehrani L, Roppe J, Schweiger E, Smith ND, Anderson J, Bristow L, Brodkin J, Jiang X, McDonald I, et al. (2003) 3-[(2-Methyl-1,3-thiazol-4-yl)ethynyl]pyridine: a potent and highly selective metabotropic glutamate subtype 5 receptor antagonist with anxiolytic activity. *J Med Chem* **46:**204–206.

Dölen G, Osterweil E, Rao BS, Smith GB, Auerbach BD, Chattarji S, and Bear MF (2007) Correction of fragile X syndrome in mice. *Neuron* **56:**955–962.

Dringen R (2000) Metabolism and functions of glutathione in brain. *Prog Neurobiol* **62:**649–671.

Gasparini F, Lingenhöhl K, Stoehr N, Flor PJ, Heinrich M, Vranesic I, Biollaz M, Allgeier H, Heckendorn R, Urwyler S, et al. (1999) 2-Methyl-6-(phenylethynyl)-pyridine (MPEP), a potent, selective and systemically active mGlu5 receptor antagonist. *Neuropharmacology* **38:**1493–1503.

Grant FD, Fahey FH, Packard AB, Davis RT, Alavi A, and Treves ST (2008) Skeletal PET with ^{18}F-fluoride: applying new technology to an old tracer. *J Nucl Med* **49:**68–78.

Grillo MP, Hua F, Knutson CG, Ware JA, and Li C (2003) Mechanistic studies on the bioactivation of diclofenac: identification of diclofenac-*S*-acyl-glutathione in vitro in incubations with rat and human hepatocytes. *Chem Res Toxicol* **16:**1410–1417.

Kenny PJ and Markou A (2004) The ups and downs of addiction: role of metabotropic glutamate receptors. *Trends Pharmacol Sci* **25:**265–272.

Laruelle M, Slifstein M, and Huang Y (2003) Relationships between radiotracer properties and image quality in molecular imaging of the brain with positron emission tomography. *Mol Imaging Biol* **5:**363–375.

Lash LH, Qian W, Putt DA, Jacobs K, Elfarra AA, Krause RJ, and Parker JC (1998) Glutathione conjugation of trichloroethylene in rats and mice: sex-, species-, and tissue-dependent differences. *Drug Metab Dispos* **26:**12–19.

Lazarova N, Siméon FG, Musachio JL, Lu S, and Pike VW (2007) Integration of a microwave reactor with Synthia to provide a fully automated radiofluoridation module. *J Label Compd Radiopharm* **50:**463–465.

Li X, Need AB, Baez M, and Witkin JM (2006) Metabotropic glutamate 5 receptor antagonism is associated with antidepressant-like effects in mice. *J Pharmacol Exp Ther* **319:**254–259.

Ma Y, Lang L, Kiesewetter DO, Jagoda E, Sassaman MB, Der M, and Eckelman WC (2001) Liquid chromatography–tandem mass spectrometry identification of metabolites of two 5-HT$_{1A}$ antagonists, *N*-{2-[4-(2-methoxylphenyl)piperazino]ethyl}-*N*-(2-pyridyl) *trans*- and *cis*-4-fluorocyclohexanecarboxamide, produced by human and rat hepatocytes. *J Chromatogr B Biomed Sci Appl* **755:**47–56.

Magata Y, Lang L, Kiesewetter DO, Jagoda EM, Channing MA, and Eckelman WC (2000) Biologically stable [^{18}F]-labeled benzylfluoride derivatives. *Nucl Med Biol* **27:**163–168.

Montine TJ, Amarnath V, Picklo MJ, Sidell KR, Zhang J, and Graham DG (2000) Dopamine mercapturate can augment dopaminergic neurodegeneration. *Drug Metab Rev* **32:**363–376.

Pietraszek M, Nagel J, Gravius A, Schäfer D, and Danysz W (2007) The role of group I metabotropic glutamate receptors in schizophrenia. *Amino Acids* **32:**173–178.

Pike VW (1993) Positron-emitting radioligands for studies—in vivo—probes for human psychopharmacology. *J Psychopharmacol* **7:**139–158.

Ridgewell RE and Abdel-Monem MM (1987) Stereochemical aspects of the glutathione *S*-transferase-catalyzed conjugations of alkyl halides. *Drug Metab Dispos* **15:**82–90.

Rinaldi R, Eliasson E, Swedmark S, and Morgenstern R (2002) Reactive intermediates and the dynamics of glutathione transferases. *Drug Metab Dispos* **30:**1053–1058.

Ryu YH, Liow JS, Zoghbi S, Fujita M, Collins J, Tipre D, Sangare J, Hong J, Pike VW, and Innis RB (2007) Disulfiram inhibits defluorination of ^{18}F-FCWAY, reduces bone radioactivity, and enhances visualization of radioligand binding to serotonin 5-HT$_{1A}$ receptors in human brain. *J Nucl Med* **48:**1154–1161.

Seidel J, Vaquero JJ, and Green MV (2003) Resolution uniformity and sensitivity of the NIH ATLAS small animal PET scanner: comparison to simulated LSO scanners without depth-of-interaction capability. *IEEE Trans Nucl Sci* **50:**1347–1350.

Sharma S and Lindsley CW (2007) Molecule of the month: a new high affinity PET tracer for the metabotropic glutamate receptor subtype 5 (mGlur5). *Curr Topics Med Chem* **7:**1541–1542.

Sidell KR, Montine KS, Picklo MJ Sr, Olsen SJ, Amarnath V, and Montine TJ (2003) Mercapturate metabolism of 4-hydroxy-2-nonenal in rat and human cerebrum. *J Neuropathol Exp Neurol* **62:**146–153.

Siméon FG, Brown AK, Zoghbi SS, Patterson VM, Innis RB, and Pike VW (2007) Synthesis and simple ^{18}F-labeling of 3-fluoro-5-(2-(2-(fluoromethyl)thiazol-4-yl)ethynyl)benzonitrile as a high affinity radioligand for imaging monkey brain metabotropic glutamate subtype-5 receptors with positron emission tomography. *J Med Chem* **50:**3256–3266.

Soiefer AI and Kostyniak PJ (1984) Purification of a fluoroacetate-specific defluorinase from mouse liver cytosol. *J Biol Chem* **259:**10787–10792.

Tecle B and Casida JE (1989) Enzymatic defluorination and metabolism of fluoroacetate, fluoroacetamide, fluoromethanol, and (−)-erythro-fluorocitrate in rats and mice examined by ^{19}F and ^{13}C NMR. *Chem Res Toxicol* **2:**429–435.

Teitelbaum PJ, Chu NI, Cho D, Tökés L, Patterson JW, Wagner PJ, and Chaplin MD (1981) Mechanism for the oxidative defluorination of flunisolide. *J Pharmacol Exp Ther* **218:**16–22.

Tipre DN, Zoghbi SS, Liow JS, Green MV, Seidel J, Ichise M, Innis RB, and Pike VW (2006) PET imaging of brain 5-HT_{1A} receptors in rat in vivo with ^{18}F-FCWAY and improvement by successful inhibition of radioligand defluorination with miconazole. *J Nucl Med* **47:**345–353.

Tsai VW, Scott HL, Lewis RJ, and Dodd PR (2005) The role of group I metabotropic glutamate receptors in neuronal excitotoxicity in Alzheimer's disease. *Neurotox Res* **7:**125–141.

Tu LQ, Chen YY, Wright PF, Rix CJ, Bolton-Grob R, and Ahokas JT (2005) Characterization of the fluoroacetate detoxication enzymes of rat liver cytosol. *Xenobiotica* **35:**989–1002.

Wheeler JB, Stourman NV, Armstrong RN, and Guengerich FP (2001) Conjugation of haloalkanes by bacterial and mammalian glutathione transferases: mono- and vicinal dihaloethanes. *Chem Res Toxicol* **14:**1107–1117.

Yang X and Chen W (2005) In vitro microsomal metabolic studies on a selective mGluR5 antagonist MTEP: characterization of *in vitro* metabolites and identification of a novel thiazole ring opening aldehyde metabolite. *Xenobiotica* **35:**797–809.

Address correspondence to: Dr. H. Umesha Shetty, PET Radiopharmaceutical Sciences, Molecular Imaging Branch, National Institute of Mental Health, National Institutes of Health, Bldg. 10, Rm B3 C351, 10 Center Dr., MSC 1003, Bethesda, MD 20892-1003. E-mail: shettyu@mail.nih.gov